

# Finite Element Analysis of Two Different Implant Applicable for Vertical Bone Deficiency at Maxillary Sinus

Mert Atao<sup>1,\*</sup>, Adnan Kilinc<sup>2</sup>, Nesrin Saruhan<sup>3</sup>, and Mustafa Gundogdu<sup>4</sup>

<sup>1</sup>Department of Oral and Maxillofacial Surgery, Faculty of Dentistry, Mersin University, Mersin, 33340, Turkey

<sup>2</sup>Department of Oral and Maxillofacial Surgery, Faculty of Dentistry, Ataturk University, Erzurum, 25240, Turkey

<sup>3</sup>Department of Oral and Maxillofacial Surgery, Faculty of Dentistry, Osmangazi University, Eskisehir, 26040, Turkey

<sup>4</sup>Department of Prosthodontics, Faculty of Dentistry, Ataturk University, Erzurum, 25240, Turkey

**Objective:** The critical point of the sinus floor elevation procedure is retaining the membrane intact. The BoneTrust Sinus© (BTS) implant system is recommended by the manufacturer as it could protect the membrane from perforation and provide greater primary stability. The aim of this study was to evaluate the stress distribution on the surrounding bone and implant body of this implant design compared with the conventional BoneTrust Plus© (BTP) design using three-dimensional (3D) finite element analyses (FEAs). **Study Design:** Six different finite element models, including two implant designs of three different graft qualities (high-stiff, medium-stiff and low-stiff), were prepared for the implant surgery on an atrophic edentulous maxilla with sinus pneumatization of a healthy individual. Then, these models were loaded with vertical and 30° oblique forces. With 3D FEAs, stress distributions of these models were obtained, color-coded, and shown numerically. **Results:** According to the results of the study, oblique loading caused higher stress than vertical loading. The stresses were highest in the crestal cortical bone, lower in the graft, and lowest in the trabecular bone. In addition, BTS implant design had similar stress distribution values on the implant body, the surrounding bone, and the graft as did the conventional BTP design. **Conclusions:** The BTS implant design could be effective in stress distribution similarly to the conventional design and could even be preferable because of its clinical advantages. Additionally, these are obtained that supported cortical bone thickness, graft quality and angular parallelism between implants and occlusal forces are important factors in terms of load-bearing capacity.

**Keywords:** Finite Element Analysis, Sinus Floor Elevation, Sinus Membrane Perforation, Sinus Grafting, Dental Implant.

## 1. INTRODUCTION

In terms of implant surgery, the posterior edentulous maxilla requires a unique perspective, different from the other regions of the mouth. In this region, the most significant challenge is the presence of the maxillary sinus.<sup>1</sup> After a tooth extraction, the combination of continuing loss of bone height and antral pneumatization could decrease the subantral bone height.<sup>2</sup> If the bone height is insufficient for dental implant placement, the preferred option for correcting this condition is maxillary sinus floor elevation.<sup>3,4</sup> Incidentally, it is possible to regenerate the vertical bone loss with bone grafts or bone tissue regeneration materials and ensure suitable bone support for dental implants.<sup>5,6</sup>

The maxillary sinus is a pyramidal-shaped air cavity, which is bilaterally located in the maxilla. It could include internal vertical septa that separate sinus cavity.

The alveolar bone has a thick external cortex and a thin internal cortex. Trabecular bone is situated between the cortical plates. The sinus is lined by a very thin, pseudostriated, ciliated epithelium that is called the Schneiderian membrane. This membrane allows the passage of fluids towards the nasal cavity.<sup>2</sup>

This is the critical challenge of the sinus floor elevation procedure—the Schneiderian membrane must remain intact throughout the entire operation. Nevertheless, if there is a sinus membrane perforation during the surgery, the planned sinus floor elevation procedure must be halted and the perforation has to be repaired or the procedure must be postponed.<sup>7</sup> There are various techniques, materials and armamentarium to use for managing this complication. Even so, the most efficient approach for the management of sinus perforation is prevention.

One of the current products produced for this procedure is the “BoneTrust Sinus” implant system (Medical Instinct

\*Author to whom correspondence should be addressed.

Zahn Implantate, Boven, Germany). In conventional sinus elevation procedure, after the sinus membrane is elevated and sinus floor is grafted from a lateral bone window, a standard screw design implant was placed.<sup>2</sup> While there is a possibility that the sharp surfaces of the implant may perforate the sinus membrane during placement of screw design implants,<sup>8</sup> according to the manufacturer's literature, this system protects the membrane from perforation, provides a greater primary stability and allows a one-step sinus floor elevation procedure (simultaneous augmentation and implantation).

The finite element analyses (FEA) was developed for use in the aerospace research in the early 1960s and after a while, it was used in the field of implantology.<sup>9–11</sup> Contemporarily, several studies in implantology research have used computational, analytical, and experimental models, by means of, especially finite element analysis.<sup>12–16</sup>

The aim of this study was to evaluate the stress distribution on the surrounding bone of two different implant designs which were applicable for vertical bone deficiency at the maxillary sinus region with three-dimensional (3D) finite element analyses (FEAs) and to investigate the effect of graft quality used for sinus lifting on the stress distribution around the implants.

## 2. MATERIALS AND METHODS

The geometry of the maxilla was defined by cone beam computed tomography data of the atrophic edentulous maxilla with sinus pneumatization of a healthy individual. The residual bone height used for modeling was 7 mm. The alveolar ridge width used for the model was 6 mm. The external (crestal) cortical thickness was assumed to be 1 mm, the trabecular bone thickness was 5.5 mm and inner cortical bone thickness was 0.5 mm throughout. A 7 mm grafted sinus area was modeled. Single implants were modeled by using the company catalog, placed in the center of the 3D reconstruction in all cases and then inclined 12° away from the horizontal plane to mimic a clinical situation. All components used in the model were assumed to be linearly elastic, isotropic and homogenous (Fig. 1).

The graft stiffness and implant designs were modeled to simulate six different clinical conditions as shown in Figure 5.

Three different graft qualities were studied and described as follows:

- High-stiff graft,
- Medium-stiff graft and
- Low-stiff graft.<sup>11</sup>

Two different implant designs were grouped and are shown in Figure 2; they are named as follows:

- *Group 1:* (BTS) Medical Instinct BoneTrust® Sinus 4 mm diameter/12 mm length cylindrical titanium implant (6.5 mm threaded/5.5 mm non-threaded special design) and

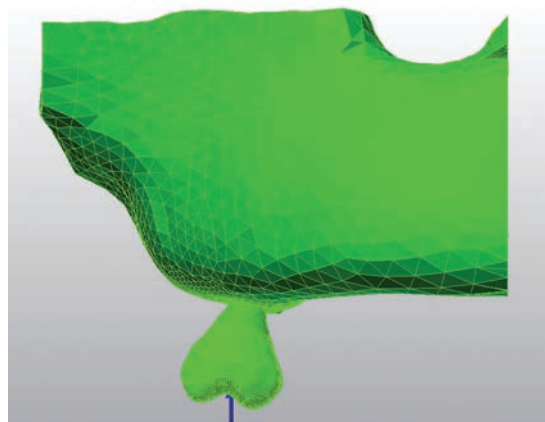


Fig. 1. Three-dimensional finite element model of all structures.

- *Group 2:* (BTP) Medical Instinct BoneTrust® Plus 4 mm diameter/11.5 mm length cylindrical titanium implant.

For both implant designs, abutment (Medical Instinct Direct Abutment) with 0° inclination, 4.0 mm diameter and 3 mm gingival height) and standardized upper first molar full-ceramic restoration was modeled by using the company catalog. The Group 1 model meshed with 75241 nodes and 401689 elements, and the Group 2 model meshed with 91372 nodes and 499254 elements.

Young's modulus and Poisson's ratio of all components used in the analysis were defined according to the current literature<sup>11,17</sup> and are shown in Table I.



Fig. 2. Two different implant designs: A—BoneTrust Plus; B—BoneTrust Sinus.



**Table I.** Young's modulus and poisson's ratio of studied components.

	Young's modulus (GPa)	Poisson's ratio
Titanium (implant and abutment)	110	0.35
Cortical bone	13.7	0.30
Trabecular bone	1.37	0.30
Full ceramic restoration	95	0.2
Graft high stiff	11	0.3
Graft medium stiff	5	0.3
Graft low stiff	0.2	0.3

To simulate occlusion, implants were mechanically loaded at full-ceramic restoration with a defined force of 300 N vertical and 300 N inclined 30° posteriorly relative to the implant axis at the buccal surface of the mesiolingual cusp.<sup>18–20</sup> These simulations generated a spatial force that acted on the implant body.

The 3D finite element pre- and postprocessing software used to construct the finite element models and to evaluate the stresses were as follows: Activity 880 (Smart Optics Sensortechnik GmbH, Bochum, Germany) for optical scanning and Rhinoceros 4.0 (Robert Mc Neel and Associates, Seattle, WA, USA) for 3D modeling. Linear static finite element analysis of stress distributions of the bone implant system was computed with the Algor Fempro finite element software package (Algor, Inc., Pittsburgh, PA, USA) and VRMesh Studio (VirtualGrid Inc., Bellevue City, WA, USA). Data for the cortical stresses (von Mises stress values) were obtained in MPa, color-coded and shown numerically.

### 3. RESULTS

Figures 3 and 4 show the von Mises stress distribution in MPa within the implant and abutment under vertical and oblique loading. Stress values in MPa within the implant and abutment under oblique loading were more than those under vertical loading independent of all the factors (Table II). In the vertical loading, the stress distribution was concentrated in the buccal bone region, and oblique loading was concentrated in the palatal bone region (Tables III, IV).

The maximum von Mises stress values on implant and abutment were observed near the implant and abutment connection; associatively, the maximum von Mises stress values on bone were observed in the cortical bone adjacent to the implant neck for all factors tested (loading direction, implant design, and graft quality) (Figs. 3, 4) (Tables III, IV).

Tables III and IV show a linear relationship between graft quality and the load-bearing capacity of the graft type. In relation to graft quality, the von Mises stress values on cortical and trabecular bones decreased. Regarding the grafted bone, the stress was highest at the first thread and decreased in the subsequent threads.

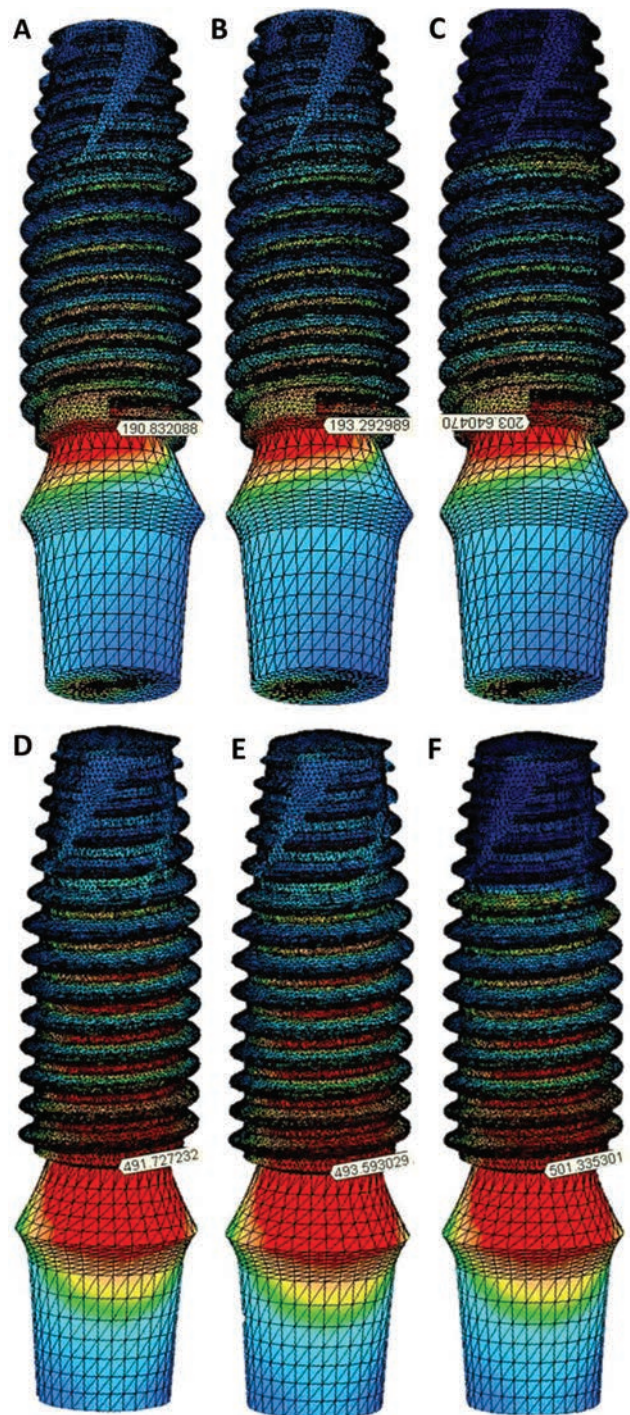


**Fig. 3.** Stress distribution on the BoneTrust Plus implant and abutment body: A—Vertical high-stiff, B—Vertical medium-stiff, C—Vertical low-stiff, D—Oblique high-stiff, E—Oblique Medium-stiff and F—Oblique low-stiff.

### 4. DISCUSSION

Biomechanical factors, basically implant design, have an impact on the implant's stability. The main argument for primary stability is mechanical fixation by the implant threads.<sup>21</sup> It is known that the mechanisms of stress distribution and load transfer to the implant-bone interface are



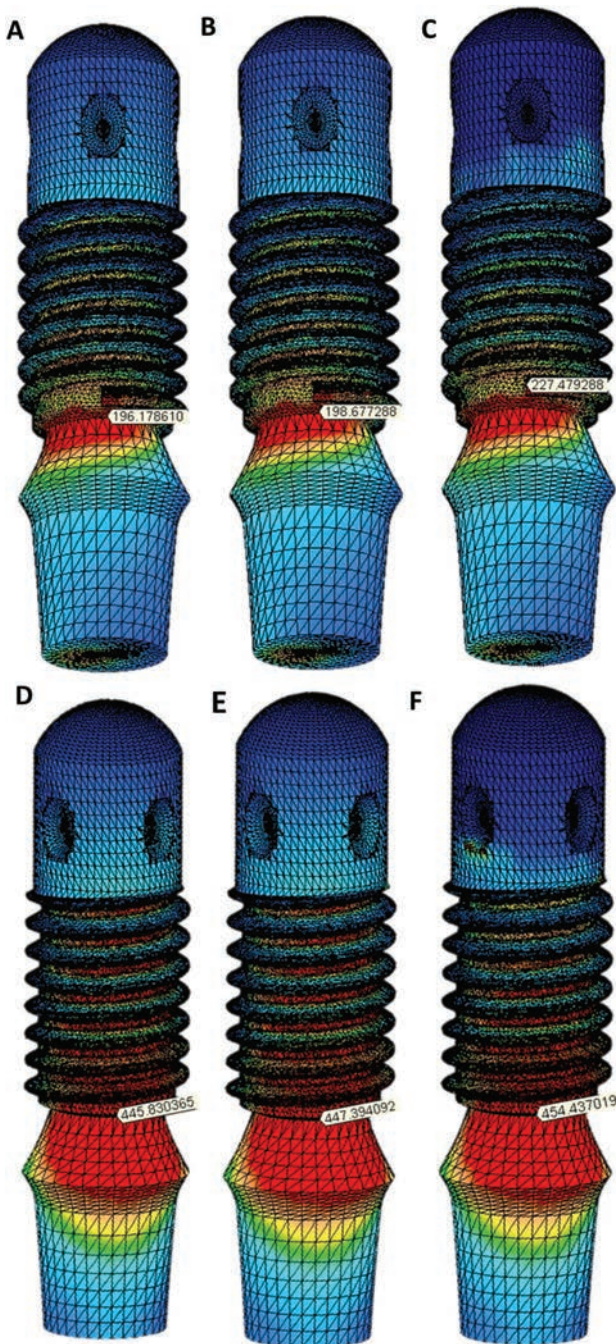


**Fig. 4.** Stress distribution on the BoneTrust Sinus implant and abutment body: A—Vertical high-stiff, B—Vertical medium-stiff, C—Vertical low-stiff, D—Oblique high-stiff, E—Oblique medium-stiff and F—Oblique low-stiff.

critical issues that can affect the success rate of implants.<sup>22</sup> It has been suggested that loading is the most critical factor in determining the long-term success of dental implants.<sup>23</sup>

Direct clinical evaluation (immediate or longitudinal) is the most reliable method to use in order to analyze the biomechanical response to the mechanical loading of endosseous implants. However, the complexity of the structures involved makes a direct clinical evaluation of the

**Table II.** Stress values on implant body and abutment in MPa.

Force	BoneTrust plus			BoneTrust sinus		
	High	Medium	Low	High	Medium	Low
Oblique	491.7272	493.5930	501.3353	445.8303	447.3940	454.4370
Vertical	190.8320	193.2929	203.6404	196.1786	198.6772	227.4792

biomechanical behavior of intraosseous structures nearly impossible, considering the difficulty of the methodology, potential ethical issues and the long period of time required for this type of study. To overcome these limitations, several studies have used computational, analytical and experimental models, such as the frequently used FEA to evaluate the biomechanics of dental implants.<sup>9</sup>

In this study, 3D FEA was used to evaluate stress distribution on the surrounding bone of two different implant designs and to investigate the effect of quality used for sinus lifting.

According to the results of this study, oblique loading causes much more stress in both the implant body and bone components compared to vertical loading for both implant designs (Tables II–IV) in accordance with the current literature.<sup>24–26</sup> As titanium alloys are known to tolerate the stress of up to 900 MPa without irreversible deformation,<sup>5</sup> the maximum stress of 501 N applied to the implant is unlikely to cause implant failure (Table II).

In the vertical loading, the stress distribution was concentrated in the buccal bone region due to the implant placement at 12° angulation to simulate clinical conditions. On the other hand, in oblique loading, due to the force loaded on the palatal cusp, which is the functional cusp, stress distribution was concentrated in the palatal bone region (Tables III, IV), in accordance with the current literature.<sup>24, 26</sup>

It was interesting that comparative analysis of the stress distribution patterns in the studied models suggested that oblique loading produced significantly higher stress concentrations in the upper portion of the implant compared to vertical loading. However, there was no significant difference in the stresses in the apical portion of the implant between the two different loading directions (Tables III, IV).

Maximum von Mises stress values were observed near the implant and abutment connection for all factors tested (loading direction, implant design, and graft quality) (Figs. 3, 4). Similarly, Sevimay et al.<sup>18</sup> and Koca et al.<sup>20</sup> demonstrated the highest values at the neck of the implant.

There was no difference in stress distributions between the *BTS* and *BTP* implant designs. The stress values were evaluated, and it was determined that there was a decrease in the stress values of the *BTS* implant in 29 of 108 (74%) of the parameters evaluated at oblique loading and in 41 of 108 (62%) of the parameters evaluated at vertical loading (Tables III, IV). These results were interpreted to mean

**Table III.** Stress values of two different implant designs on cortical and trabecular bone and graft types with vertical loading in MPa.

	High				Medium				Low			
	M	D	B	P	M	D	B	P	M	D	B	P
<b>BTS</b>												
Cortical												
Von Mises	7.3907	13.5308	23.8803	5.4015	7.8281	14.2744	25.0322	5.0267	9.8977	17.3602	29.9615	4.5604
Max. Princ.	0.7567	0.1526	2.1288	4.0734	0.7106	0.1546	2.2922	3.2521	0.7624	0.1988	2.9980	0.5915
Min. Princ.	-7.3769	-14.9870	-24.5192	-2.0237	-7.9788	-15.9186	-25.6974	-2.5092	-10.4523	-19.6015	-30.7069	-4.2262
Trabecular												
Von Mises	1.1948	1.4839	2.8492	0.7284	1.3519	1.6757	3.0683	0.8093	1.9715	2.4071	4.0231	1.3019
Max. Princ.	0.5769	0.6426	1.4236	0.5364	0.6651	0.7614	1.5977	0.7307	1.0226	1.2132	2.3824	1.5667
Min. Princ.	-0.7867	-1.0457	-1.7945	-0.2781	-0.8798	-1.1490	-1.8779	-0.1635	-1.2360	-1.5401	-2.2114	0.1555
Graft												
Von Mises	4.1485	2.2649	3.5872	3.1975	3.0226	1.9704	2.8598	2.5750	0.4083	0.2932	0.4805	0.3088
Max. Princ.	1.0098	0.6383	0.8563	0.7245	1.3009	0.8927	1.2748	0.8660	0.3899	0.1957	0.4128	0.1700
Min. Princ.	-3.6878	-1.9512	-3.2470	-2.9021	-2.1615	-1.3748	-2.0189	-2.0666	-0.0791	-0.1419	-0.1409	-0.1824
<b>BTP</b>												
Cortical												
Von Mises	7.3734	13.9246	24.5073	5.2945	7.8111	14.6849	25.7136	4.9421	9.7446	17.5922	30.4700	4.5525
Max. Princ.	0.7751	0.2662	2.2877	3.8548	0.7088	0.2900	2.4611	3.0382	0.7697	0.3907	3.1486	0.5143
Min. Princ.	-7.2954	-15.3275	-25.1721	-2.1481	-7.8950	-16.2661	-26.4037	-2.6424	-10.1954	-19.6947	-31.2319	-4.2660
Trabecular												
Von Mises	1.2122	1.5040	2.9143	0.7404	1.3727	1.6973	3.1369	0.8280	1.5848	2.3656	4.0250	1.2715
Max. Princ.	0.5498	0.6196	1.3411	0.5357	0.6374	0.7394	1.5068	0.7222	0.9780	1.1574	2.1921	1.4530
Min. Princ.	-0.8324	-1.0903	-1.9296	-0.2936	-0.9296	-1.1943	-2.0253	-0.1961	-0.8476	-1.5466	-2.3801	0.0663
Graft												
Von Mises	4.1576	2.6466	3.8558	3.2856	3.0059	2.2325	3.1053	2.7300	0.3864	0.2898	0.4755	0.2804
Max. Princ.	0.8179	0.6304	0.9024	0.6206	1.0828	0.8919	1.3028	0.4822	0.3344	0.1792	0.3788	0.1261
Min. Princ.	-3.8460	-2.3961	-3.5027	-3.0725	-2.3330	-1.6783	-2.2660	-2.5969	-0.1109	-0.1545	-0.1698	-0.1889

**Table IV.** Stress values of two different implant designs on cortical and trabecular bone and graft types with oblique loading in MPa.

	High				Medium				Low			
	M	D	B	P	M	D	B	P	M	D	B	P
<b>BTS</b>												
Cortical												
Von Mises	20.1072	11.7241	25.1990	29.3938	20.5473	11.4688	24.6178	30.1714	22.9427	11.6005	23.6931	33.9547
Max. Princ.	1.8894	10.3918	24.6253	0.9808	1.8426	9.8305	23.9807	1.0158	1.8373	8.9413	22.8579	1.1713
Min. Princ.	-0.2131	-2.6230	-2.9053	-31.7152	-20.8238	-2.9628	-2.9040	-32.6259	-23.7575	-4.1502	-3.0376	-36.9747
Trabecular												
Von Mises	2.5516	0.9882	2.5479	4.5601	2.7006	0.9699	2.4354	4.7479	3.3310	1.0307	2.1318	5.6627
Max. Princ.	1.0077	0.7959	1.8920	4.6219	1.1134	0.7481	1.8325	4.8942	1.5849	0.6675	1.6285	6.2558
Min. Princ.	-1.8457	-0.3319	-0.9125	-0.5349	-1.9174	-0.3557	-0.8401	-0.4687	-2.1922	-0.4683	-0.6944	-0.1071
Graft												
Von Mises	3.3328	3.0001	3.4559	3.5795	2.5066	2.0803	2.3852	2.6547	0.3848	0.2024	0.2215	0.6539
Max. Princ.	0.9218	0.3855	0.5231	0.7901	1.1720	0.5595	0.4865	1.2173	0.3730	0.0973	0.0434	0.8826
Min. Princ.	-2.8848	-2.9308	-3.3636	-3.2951	-1.7124	-1.7903	-2.1699	-1.8367	-0.0654	-0.1347	-0.1971	0.1626
<b>BTP</b>												
Cortical												
Von Mises	20.5735	12.2404	26.0256	28.4921	21.0408	12.0037	25.4421	29.2945	23.3398	12.1559	24.5515	32.8919
Max. Princ.	2.3421	11.0209	25.3189	1.1738	2.3155	10.4842	24.6702	1.2121	2.3722	9.7169	23.5741	1.3715
Min. Princ.	-20.4071	-2.4557	-3.0378	-30.7081	-21.0274	-2.8342	-3.0355	-31.6440	-23.7715	-4.0029	-3.1693	-35.7654
Trabecular												
Von Mises	2.7001	0.9711	2.5409	4.3877	2.8573	0.9588	2.4242	4.5712	3.4748	1.0299	2.1223	5.3868
Max. Princ.	1.0254	0.8085	1.9557	4.2318	1.1388	0.7649	1.8863	4.4928	1.6059	0.7026	1.6684	5.6872
Min. Princ.	-1.9903	-0.2986	-0.8155	-0.7473	-2.0645	-0.3227	-0.7486	-0.6894	-2.3295	-0.4300	-0.6197	-0.3941
Graft												
Von Mises	3.3813	3.6943	3.6078	3.7111	2.5405	2.4982	2.5040	2.7412	0.3718	0.2164	0.2269	0.6140
Max. Princ.	0.8318	0.3877	0.4119	0.9347	1.0554	0.5641	0.4168	1.3180	0.3295	0.0868	0.0372	0.7818
Min. Princ.	-3.0254	-3.6229	-3.6078	-3.3309	-1.8652	-2.2100	-2.3449	-1.8435	-0.0958	-0.1582	-0.2057	0.1009



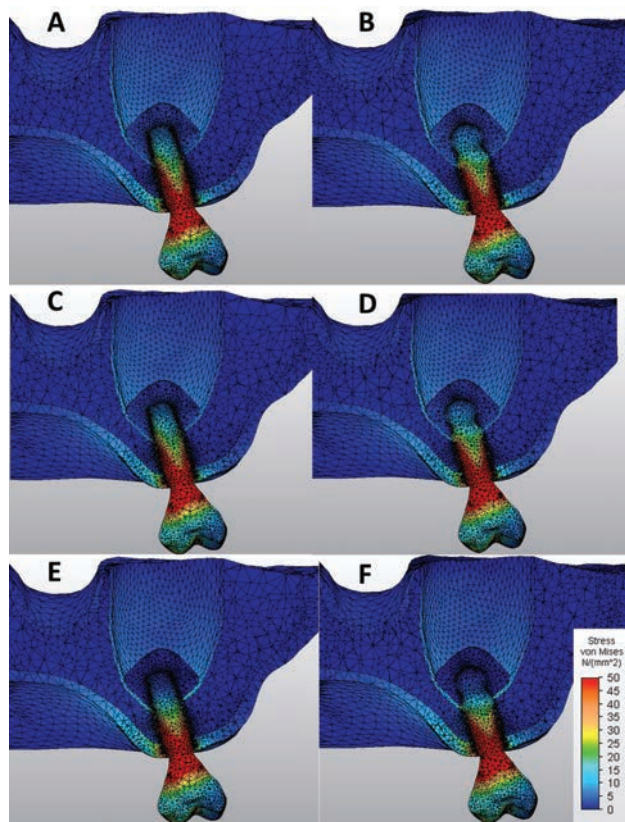


**Fig. 5.** Stress distribution of different graft stiffness on the implant and bone at oblique loading: A—BTP implant and high-stiff graft, B—BTS implant and high-stiff graft, C—BTP implant and Medium-stiff graft, D—BTS implant and medium-stiff graft, E—BTP implant and low-stiff graft, F—BTS implant and low-stiff graft.

that there was no difference in stress distribution between the two different implant designs tested.

The bone-implant interface is the primary load-bearing area in terms of stress distribution.<sup>18</sup> Many studies have shown that the maximum stress values are demonstrated within the cortical bone.<sup>18,20</sup> According to our study, maximum stresses were located within the cortical bone in contact with the implant, and especially within the palatal contour of the maxilla (Tables III, IV). Figure 5 represents the von Mises stress distributions of the entire model of two different implant designs for three different graft qualities at oblique loading. The stresses were highest in the crestal cortical bone, lower in the graft, and lowest in the trabecular bone. The stresses in the trabecular bone were at least 10 times lower for oblique loading and at least two times lower for vertical loading than those in the crestal cortical bone. However, specific stress concentration regions were noteworthy at the bottom of the trabecular layer and wedged between the thread of the implant. It is well-known that loaded implants show typical bone loss around the implant neck.<sup>27</sup> The results of the present study indicated the cause of this clinical condition.

Çehreli et al. demonstrated that the apical section of an implant was supported by grafting materials in the maxillary sinus.<sup>28</sup> Also, it has been noted that one of the important factors that affect graft quality is the maturation process. According to our study's results, which are related to those of previous reports,<sup>5,11,19</sup> as graft quality increases, the load-bearing capacity of the graft increases. Also, we found that the stress values on cortical and trabecular bones decreased for all models tested (Tables III, IV) which indicated that graft quality positively affected the stress distribution on the implant and surrounding bone.

## 5. CONCLUSIONS

In summary, within the limitations of this 3D FEA study, the results indicated the following:

- (1) Oblique loading caused higher stress than vertical loading, so the implants should be placed as parallel as possible to the occlusal forces.
- (2) The stresses were highest in the crestal cortical bone, lower in the graft, and lowest in the trabecular bone. This information confirmed that the most important parameter in terms of load-bearing capacity is cortical bone thickness around the implant.
- (3) The increase in graft quality is important for load-bearing capacity. As graft quality increases, the load-bearing capacity of the graft increases, and the stress values on cortical and trabecular bones decrease.
- (4) The *BTS* implant design had similar results when compared to conventional design. Although the surface area of the *BTS* implant is less than that of the conventional design, it is thought that after the osseointegration is achieved, this design could be effective in terms of stress distribution similar to the conventional design. It could possibly be preferable because of its clinical advantages.

**Acknowledgment:** The authors did not receive grants or any type of financial assistance from the public, commercial or not-for-profit funding agencies. The authors would like to thank Ayberk Yağız (Ay Tasarım, Ankara, Turkey) for his efforts in finite element analysis.

## References and Notes

1. M. Morand and T. Irinakis, The challenge of implant therapy in the posterior maxilla: Providing a rationale for the use of short implants. *J. Oral Implantol.* 33, 257 (2007).
2. S. V. Raja, Management of the posterior maxilla with sinus lift: Review of techniques. *J. Oral Maxillofac. Surg.* 67, 1730 (2009).
3. R. Martuscelli, P. Toti, L. Sbordone, F. Guidetti, L. Ramaglia, and C. Sbordone, Five-year outcome of bone remodelling around implants in the maxillary sinus: Assessment of differences between implants placed in autogenous inlay bone blocks and in ungrafted maxilla. *Int. J. Oral Maxillofac. Surg.* 43, 1117 (2014).
4. S. S. Wallace and S. J. Froum, Effect of maxillary sinus augmentation on the survival of endosseous dental implants. A systematic review. *Ann. Periodontol.* 8, 328 (2003).

5. G. Tepper, R. Haas, W. Zechner, W. Krach, and G. Watzek, Three-dimensional finite element analysis of implant stability in the atrophic posterior maxilla: A mathematical study of the sinus floor. *Clin. Oral Implants Res.* 13, 657 (2002).
6. C. Dalro G. de, Biomaterials for bone tissue regeneration and bone disease. *J. Bionanoscience* 12, 599 (2018).
7. P. A. Fugazzotto, Sinus floor augmentation at the time of maxillary molar extraction: Technique and report of preliminary results. *Int. J. Oral Maxillofac. Implant* 14, 536 (1999).
8. J. L. Lozada, C. Goodacre, A. J. Al-Ardah, and A. Garbacea, Lateral and crestal bone planing antrotomy: A simplified surgical procedure to reduce the incidence of membrane perforation during maxillary sinus augmentation procedures. *J. Prosthet. Dent.* 105, 147 (2011).
9. A. A. Pesqueira, M. C. Goiato, H. G. Filho, D. R. Monteiro, D. Micheline, M. Filie, and E. P. Pelizzer, Use of stress analysis methods to evaluate the. *J. Oral Implantol.* 40, 217 (2014).
10. V. E. de Souza Batista, F. R. Verri, D. A. de Faria Almeida, J. F. S. Junior, C. A. A. Lemos, and E. P. Pelizzer, Evaluation of the effect of an offset implant configuration in the posterior maxilla with external hexagon implant platform: A 3-dimensional finite element analysis. *J. Prosthet. Dent.* 118, 363 (2017).
11. S. Inglam, S. Suebnukarn, W. Tharanon, T. Apatananon, and K. Sitthiseripratip, Influence of graft quality and marginal bone loss on implants placed in maxillary grafted sinus: A finite element study. *Med. Biol. Eng. Comput.* 48, 681 (2010).
12. S. Yamaguchi, Y. Yamanishi, L. S. Machado, S. Matsumoto, N. Tovar, P. G. Coelho, V. P. Thompson, and S. Imazato, *In vitro* fatigue tests and in silico finite element analysis of dental implants with different fixture/abutment joint types using computer-aided design models. *J. Prosthodont. Res.* 62, 24 (2017).
13. G. Dimililer, S. Kücük Kurt, and S. Cetiner, Biomechanical effects of implant number and diameter on stress distributions in maxillary implant-supported overdentures. *J. Prosthet. Dent.* 119, 244 (2017).
14. Z. Gümrükçü and Y. T. Korkmaz, Influence of implant number, length, and tilting degree on stress distribution in atrophic maxilla: A finite element study. *Med. Biol. Eng. Comput.* Online, 1 (2017), DOI: 10.1007/s11517-017-1737-4.
15. H. Güngör, İ. Baran, and L. Karaagaçlıoğlu, Influence of cantilever extension and crown-to-implant ratio in posterior maxilla: A finite element analysis. *J. Biomater. Tissue Eng.* 8, 489 (2018).
16. O. Ozgul and I. D. Kocyigit, Choosing implant type for using with allogeneic bone ring graft: Guidance of stress analysis-part I. *J. Biomater. Tissue Eng.* 8, 190 (2018).
17. X. Yan, X. Zhang, J. Gao, and Y. Matsushita, Maxillary sinus augmentation without grafting material with simultaneous implant installation: A three-dimensional finite element analysis. *Clin. Implant Dent. Relat. Res.* 7, 515 (2015).
18. M. Sevimay, F. Turhan, M. A. Kılıçarslan, and G. Eskitaşcıoğlu, Three-dimensional finite element analysis of the effect of different bone quality on stress distribution in an implant-supported crown. *J. Prosthet. Dent.* 93, 227 (2005).
19. M. I. Fanuscu, H. V. Vu, and B. Poncelet, Implant biomechanics in grafted sinus: A finite element analysis. *J. Oral Implantol.* 30, 59 (2004).
20. Ö. L. Koca, G. Eskitaşcıoğlu, and A. Üşümez, Three-dimensional finite-element analysis of functional stresses in different bone locations produced by implants placed in the maxillary posterior region of the sinus floor. *J. Prosthet. Dent.* 93, 38 (2005).
21. A. Gülses, M. Ayna, H. Güçlü, M. Şençimen, M. N. Basiry, M. Gierloff, and Y. Açil, *In vitro* assessment of primary stability of bonetrust sinus implant design. *Int. J. Periodontics Restorative Dent.* 36, 730 (2016).
22. R. Skalak, Biomechanical considerations in osseointegrated prostheses. *J. Prosthet. Dent.* 49, 843 (1983).
23. S. J. Hoshaw, J. B. Brunski, and G. V. B. Cochran, Mechanical Loading of brånemark implants affects interfacial bone modeling and remodeling. *Int. J. Oral Maxillofac. Implants* 9, 345 (1994).
24. R. Sadrimanesh, H. Siadat, P. Sadr-Eshkevari, A. Monzavi, P. Maurer, and A. Rashad, Alveolar bone stress around implants with different abutment angulation. *Implant Dent.* 21, 196 (2012).
25. E. O. Almeida, E. P. Rocha, A. C. Freitas Júnior, R. B. Anchieta, R. Poveda, N. Gupta, and P. G. Coelho, Tilted and short implants supporting fixed prosthesis in an atrophic maxilla: A 3D-FEA biomechanical evaluation. *Clin. Implant Dent. Relat. Res.* 17, 332 (2015).
26. B. R. Chrcanovic, T. Albrektsson, and A. Wennerberg, Tilted versus axially placed dental implants: A meta-analysis. *J. Dent.* 43, 149 (2015).
27. L. Laurell and D. Lundgren, Marginal bone level changes at dental implants after 5 years in function: A meta-analysis. *Clin. Implant Dent. Relat. Res.* 13, 19 (2011).
28. M. C. Çehrelı, M. Akkocaoğlu, A. Comert, I. Tekdemir, and K. Akça, Bone strains around apically free versus grafted implants in the posterior maxilla of human cadavers. *Med. Bio. Eng. Comput.* 45, 395 (2007).

Received: 17 January 2019.